

# Stochastic and Tensor Network simulations of the Hubbard Model

Johann Ostmeyer

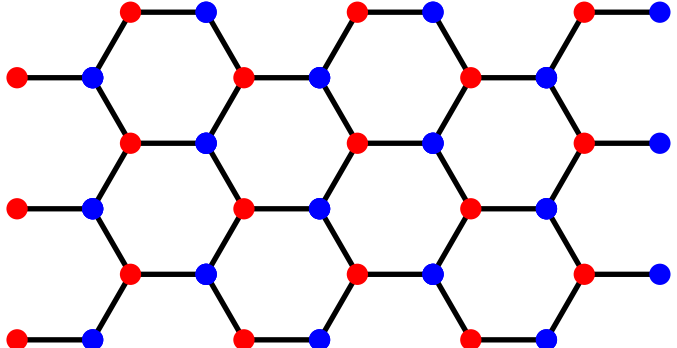
Department of Mathematical Sciences, University of Liverpool, United Kingdom

August 13, 2022



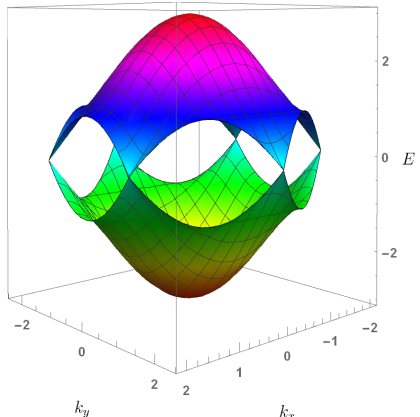
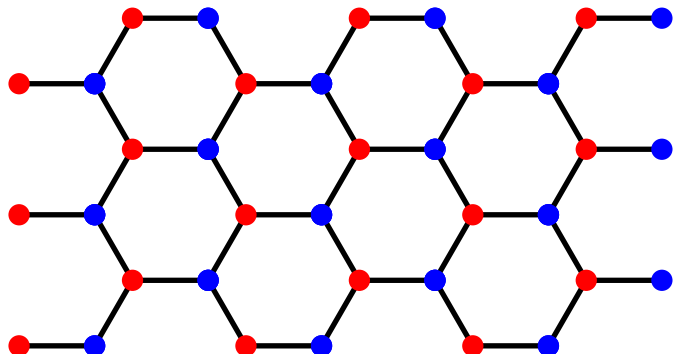
Hubbard model [Hubbard *ProcRSoc* **276** (1963); Wallace *PhysRev* **71** (1947)]

$$H = - \sum_{\langle x,y \rangle, s} c_{x,s}^\dagger c_{y,s}$$



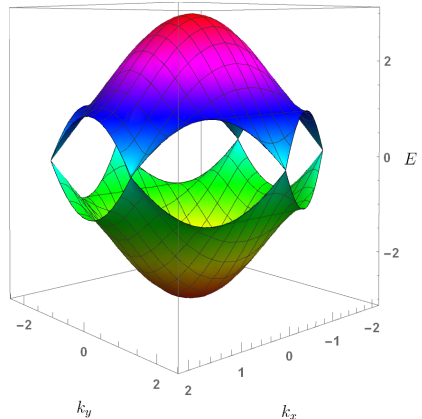
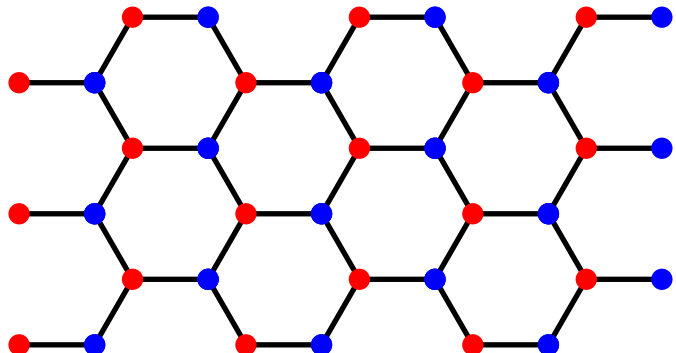
Hubbard model [Hubbard *ProcRSoc* **276** (1963); Wallace *PhysRev* **71** (1947)]

$$H = - \sum_{\langle x,y \rangle, s} c_{x,s}^\dagger c_{y,s}$$

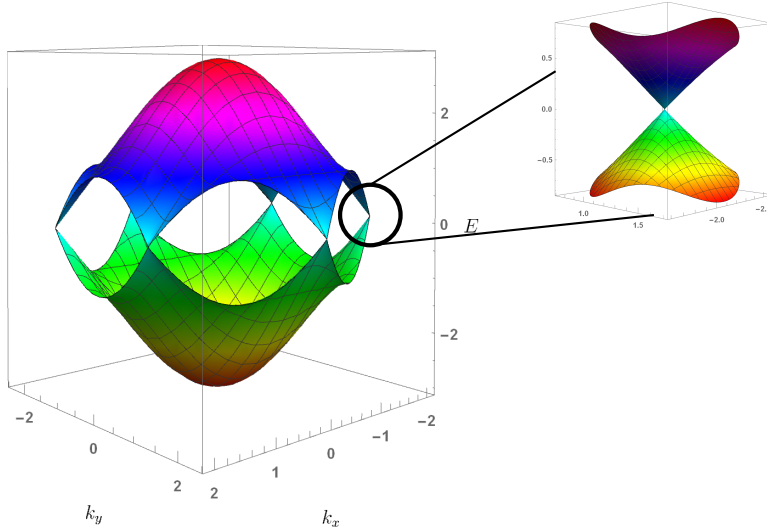


Hubbard model [Hubbard *ProcRSoc* **276** (1963); Wallace *PhysRev* **71** (1947)]

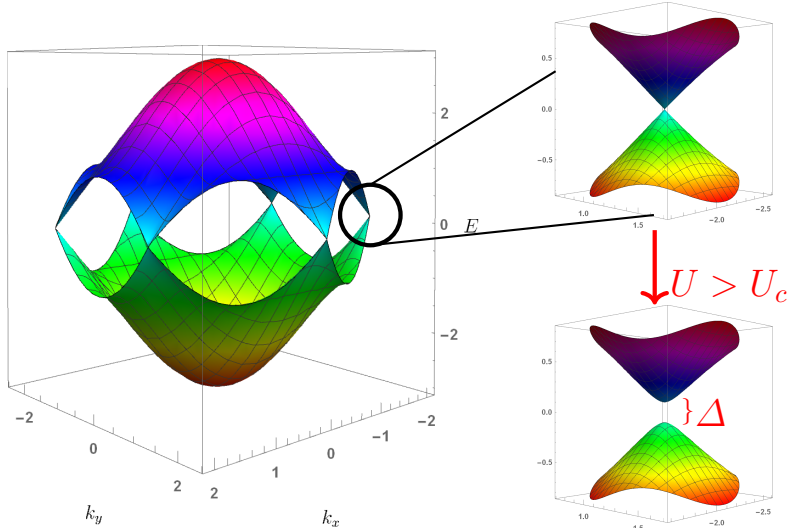
$$H = - \sum_{\langle x,y \rangle, s} c_{x,s}^\dagger c_{y,s} + \frac{1}{2} U \sum_x q_x^2$$



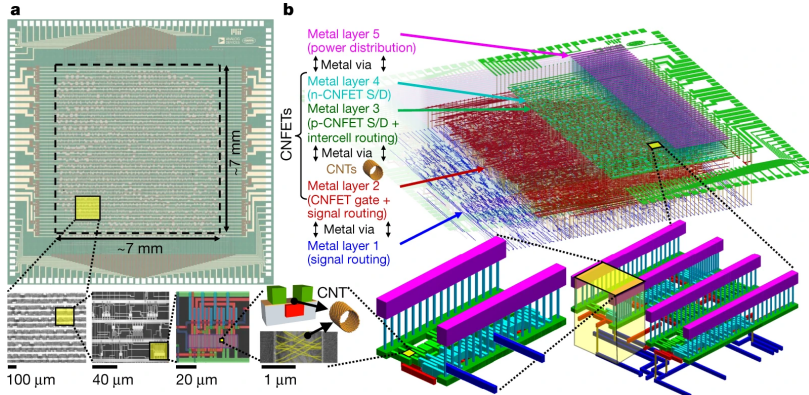
# Expected phase transition



## Expected phase transition



# Carbon Nanotube computer



“Hello, world!  
I am RV16XNano.”

[Hills *et al.* *Nature* **572** (2019)]

Path integral formalism [Krieg, JO et al. *CPC* **236** (2019); Luu & Lähde *PRB* **93** (2016)]

- ▶ Discretise imaginary time into steps  $\delta = \beta/N_t$ ,  $\beta = 1/T$

Path integral formalism [Krieg, JO et al. *CPC* **236** (2019); Luu & Lähde *PRB* **93** (2016)]

- ▶ Discretise imaginary time into steps  $\delta = \beta/N_t$ ,  $\beta = 1/T$
- ▶ Particle-hole transformation

$$p_x^\dagger \equiv c_{x,\uparrow}^\dagger, p_x \equiv c_{x,\uparrow}, h_x^\dagger \equiv c_{x,\downarrow}^\dagger, h_x \equiv c_{x,\downarrow}^\dagger$$

Path integral formalism [Krieg, JO et al. *CPC* **236** (2019); Luu & Lähde *PRB* **93** (2016)]

- ▶ Discretise imaginary time into steps  $\delta = \beta/N_t$ ,  $\beta = 1/T$
- ▶ Particle-hole transformation

$$p_x^\dagger \equiv c_{x,\uparrow}^\dagger, p_x \equiv c_{x,\uparrow}, h_x^\dagger \equiv c_{x,\downarrow}^\dagger, h_x \equiv c_{x,\downarrow}^\dagger$$

- ▶ Hubbard-Stratonovich transformation

$$e^{-\frac{1}{2} \sum_{x,y} V_{x,y} q_x q_y} \propto \int \mathcal{D}\phi_t e^{-\frac{1}{2} \sum_{x,y} V_{x,y}^{-1} \phi_{x,t} \phi_{y,t} + i \sum_x \phi_{x,t} q_x}$$

Path integral formalism [Krieg, JO et al. *CPC* **236** (2019); Luu & Lähde *PRB* **93** (2016)]

- ▶ Discretise imaginary time into steps  $\delta = \beta/N_t$ ,  $\beta = 1/T$
- ▶ Particle-hole transformation

$$p_x^\dagger \equiv c_{x,\uparrow}^\dagger, p_x \equiv c_{x,\uparrow}, h_x^\dagger \equiv c_{x,\downarrow}^\dagger, h_x \equiv c_{x,\downarrow}^\dagger$$

- ▶ Hubbard-Stratonovich transformation

$$e^{-\frac{1}{2} \sum_{x,y} V_{x,y} q_x q_y} \propto \int \mathcal{D}\phi_t e^{-\frac{1}{2} \sum_{x,y} V_{x,y}^{-1} \phi_{x,t} \phi_{y,t} + i \sum_x \phi_{x,t} q_x}$$

- ▶ Fermion matrix

$$M_{(x,t)(y,t')} = \delta_{xy} \delta_{tt'} - e^{-i \delta \cdot \phi_{x,t}} \delta_{xy} \delta_{t-1,t'} - \delta \cdot \delta_{\langle x,y \rangle} \delta_{t-1,t'}$$

Path integral formalism [Krieg, JO et al. *CPC* **236** (2019); Luu & Lähde *PRB* **93** (2016)]

- ▶ Discretise imaginary time into steps  $\delta = \beta/N_t$ ,  $\beta = 1/T$
- ▶ Particle-hole transformation

$$p_x^\dagger \equiv c_{x,\uparrow}^\dagger, p_x \equiv c_{x,\uparrow}, h_x^\dagger \equiv c_{x,\downarrow}^\dagger, h_x \equiv c_{x,\downarrow}^\dagger$$

- ▶ Hubbard-Stratonovich transformation

$$e^{-\frac{1}{2} \sum_{x,y} V_{x,y} q_x q_y} \propto \int \mathcal{D}\phi_t e^{-\frac{1}{2} \sum_{x,y} V_{x,y}^{-1} \phi_{x,t} \phi_{y,t} + i \sum_x \phi_{x,t} q_x}$$

- ▶ Fermion matrix

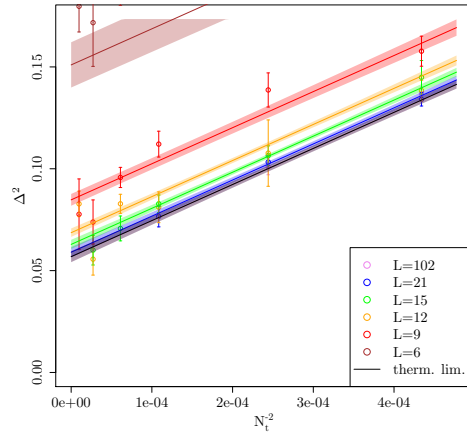
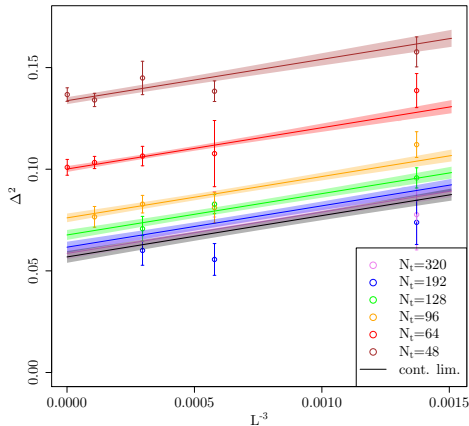
$$M_{(x,t)(y,t')} = \delta_{xy} \delta_{tt'} - e^{-i \delta \cdot \phi_{x,t}} \delta_{xy} \delta_{t-1,t'} - \delta \cdot \delta_{\langle x,y \rangle} \delta_{t-1,t'}$$

- ▶ **Hybrid Monte Carlo** simulation according to probability density

$$p[\phi] \equiv e^{-S[\phi]} = \det(M M^\dagger) e^{-\frac{\delta}{2U} \phi^2}$$

# Extrapolation towards the physical limit [JO, Berkowitz *et al.* *PRB* **102** (2020)]

$$\Delta^2 = \Delta_0^2 + c_T N_t^{-2} + c_L L^{-3}$$



Data collapse [Herbut *et al.* *PRB* **79** (2009); JO, Berkowitz *et al.* *PRB* **104** (2021)]

$$\Delta \sim \beta^{-1}$$

Data collapse [Herbut *et al.* *PRB* **79** (2009); JO, Berkowitz *et al.* *PRB* **104** (2021)]

$$\Delta \sim \beta^{-1}$$

$$\Delta \sim (U - U_c)^\nu$$

Data collapse [Herbut *et al.* *PRB* **79** (2009); JO, Berkowitz *et al.* *PRB* **104** (2021)]

$$\Delta \sim \beta^{-1}$$

$$\Delta \sim (U - U_c)^\nu$$

$$\Delta = \beta^{-1} F(\beta^{1/\nu}(U - U_c))$$

Data collapse [Herbut *et al.* *PRB* **79** (2009); JO, Berkowitz *et al.* *PRB* **104** (2021)]

$$\Delta \sim \beta^{-1}$$

$$\Delta \sim (U - U_c)^\nu$$

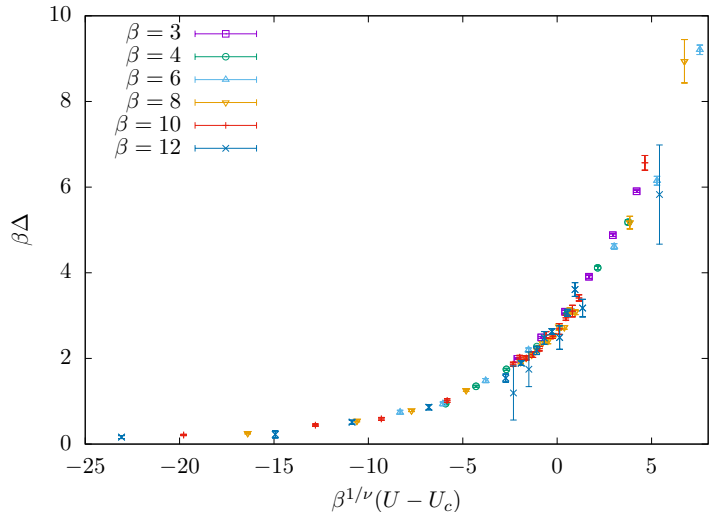
$$\Delta = \beta^{-1} F(\beta^{1/\nu}(U - U_c))$$

Data collapse [Herbut *et al.* *PRB* **79** (2009); JO, Berkowitz *et al.* *PRB* **104** (2021)]

$$\Delta \sim \beta^{-1}$$

$$\Delta \sim (U - U_c)^\nu$$

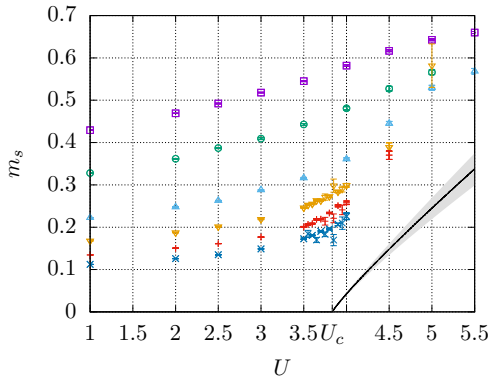
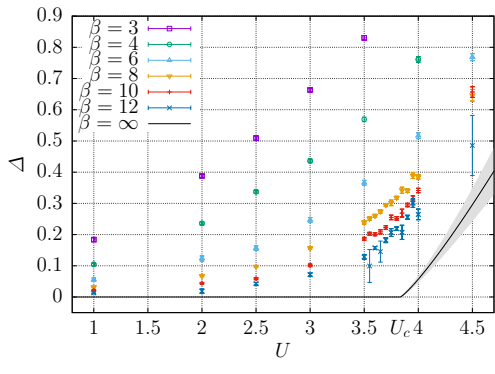
$$\Delta = \beta^{-1} F(\beta^{1/\nu}(U - U_c))$$



$$\Rightarrow U_c = 3.834(14) , \quad \nu = 1.185(43) , \quad \beta = 1.095(37)$$

# Quantum phase transition at half filling

$$H = - \sum_{\langle x,y \rangle, s} c_{x,s}^\dagger c_{y,s} + \frac{1}{2} U \sum_x q_x^2$$



Beyond half filling?

Sign problem!

$$H = - \sum_{\langle x,y \rangle, s} c_{x,s}^\dagger c_{y,s} + \frac{1}{2} U \sum_x q_x^2 + \mu \sum_x q_x$$

Beyond half filling?

Sign problem!

$$H = - \sum_{\langle x,y \rangle, s} c_{x,s}^\dagger c_{y,s} + \frac{1}{2} U \sum_x q_x^2 + \mu \sum_x q_x$$

$$p[\phi] \propto \det(M[\phi, \mu] M[\phi, -\mu]^\dagger) \not\geq 0$$

Beyond half filling?

Sign problem!

$$H = - \sum_{\langle x,y \rangle, s} c_{x,s}^\dagger c_{y,s} + \frac{1}{2} U \sum_x q_x^2 + \mu \sum_x q_x$$

$$p[\phi] \propto \det(M[\phi, \mu] M[\phi, -\mu]^\dagger) \not\geq 0$$

- Reweighting:  $\langle O \rangle = \frac{\langle O e^{i\theta} \rangle}{\langle e^{i\theta} \rangle}$

Beyond half filling?

Sign problem!

$$H = - \sum_{\langle x,y \rangle, s} c_{x,s}^\dagger c_{y,s} + \frac{1}{2} U \sum_x q_x^2 + \mu \sum_x q_x$$

$$p[\phi] \propto \det(M[\phi, \mu] M[\phi, -\mu]^\dagger) \not\geq 0$$

- ▶ Reweighting:  $\langle O \rangle = \frac{\langle O e^{i\theta} \rangle}{\langle e^{i\theta} \rangle}$
- ▶ Lefschetz Thimbles & Holomorphic Flow

[Alexandru *et al.* *PRD* **93** (2016); Cristoforetti *et al.* *PRD* **88** (2013); Ulybyshev *et al.* *PRD* **101** (2020); Rodekamp, JO *et al.* *arXiv* **2203** (2022); Wynen, JO *et al.* *PRB* **103** (2021)]

Beyond half filling?

Sign problem!

$$H = - \sum_{\langle x,y \rangle, s} c_{x,s}^\dagger c_{y,s} + \frac{1}{2} U \sum_x q_x^2 + \mu \sum_x q_x$$

$$p[\phi] \propto \det(M[\phi, \mu] M[\phi, -\mu]^\dagger) \not\geq 0$$

- ▶ Reweighting:  $\langle O \rangle = \frac{\langle O e^{i\theta} \rangle}{\langle e^{i\theta} \rangle}$
- ▶ Lefschetz Thimbles & Holomorphic Flow  
[Alexandru *et al.* *PRD* **93** (2016); Cristoforetti *et al.* *PRD* **88** (2013); Ulybyshev *et al.* *PRD* **101** (2020); Rodekamp, JO *et al.* *arXiv* **2203** (2022); Wynen, JO *et al.* *PRB* **103** (2021)]
- ▶ Machine Learning, Density of States, Complex Langevin, Line integrals  
[talks by P. Shanahan, C. Gattringer, F. Ziegler, M. W. Hansen, M. Bauer, A. Kumar, Y. Namekawa, R. Larsen, M. Fukuma, R. Thakkar, Z. Tulipant, G. Toga]

Beyond half filling?

Sign problem!

$$H = - \sum_{\langle x,y \rangle, s} c_{x,s}^\dagger c_{y,s} + \frac{1}{2} U \sum_x q_x^2 + \mu \sum_x q_x$$

$$p[\phi] \propto \det(M[\phi, \mu] M[\phi, -\mu]^\dagger) \not\geq 0$$

- ▶ Reweighting:  $\langle O \rangle = \frac{\langle O e^{i\theta} \rangle}{\langle e^{i\theta} \rangle}$
- ▶ Lefschetz Thimbles & Holomorphic Flow  
[Alexandru *et al.* *PRD* **93** (2016); Cristoforetti *et al.* *PRD* **88** (2013); Ulybyshev *et al.* *PRD* **101** (2020); Rodekamp, JO *et al.* *arXiv* **2203** (2022); Wynen, JO *et al.* *PRB* **103** (2021)]
- ▶ Machine Learning, Density of States, Complex Langevin, Line integrals  
[talks by P. Shanahan, C. Gattringer, F. Ziegler, M. W. Hansen, M. Bauer, A. Kumar, Y. Namekawa, R. Larsen, M. Fukuma, R. Thakkar, Z. Tulipant, G. Toga]
- ▶ Tensor Networks  
[Corboz *PRB* **93** (2016); Schneider, JO *et al.* *PRB* **104** (2021); talks by T. Angelides, R. Sakai, J. Bloch, T. Kuwahara]

# Projected Entangled Pair States (PEPS)

[Orús *AnnPhys* **349** (2014); Verstraete & Cirac *arXiv* **0407066** (2004); talk by L. Funcke]

$$|\psi\rangle = \sum_{s_1} \sum_{s_2} \cdots \sum_{s_N} A_{s_1, s_2, \dots, s_N} |s_1\rangle \otimes |s_2\rangle \otimes \cdots \otimes |s_N\rangle$$

# Projected Entangled Pair States (PEPS)

[Orús *AnnPhys* **349** (2014); Verstraete & Cirac *arXiv* **0407066** (2004); talk by L. Funcke]

$$\begin{aligned} |\psi\rangle &= \sum_{s_1} \sum_{s_2} \cdots \sum_{s_N} A_{s_1, s_2, \dots, s_N} |s_1\rangle \otimes |s_2\rangle \otimes \cdots \otimes |s_N\rangle \\ &\approx \sum_{s_1} \sum_{s_2} \cdots \sum_{s_N} A_{s_1; \alpha_1}^1 A_{s_2; \alpha_1, \alpha_2}^2 \cdots A_{s_N; \alpha_{N-1}}^N |s_1\rangle \otimes |s_2\rangle \otimes \cdots \otimes |s_N\rangle \end{aligned}$$

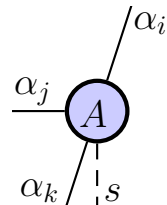
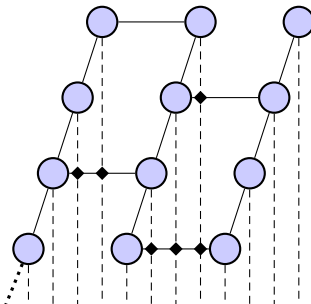
Truncate  $\alpha_i \leq D \forall i$

# Projected Entangled Pair States (PEPS)

[Orús *AnnPhys* **349** (2014); Verstraete & Cirac *arXiv* **0407066** (2004); talk by L. Funcke]

$$|\psi\rangle = \sum_{s_1} \sum_{s_2} \cdots \sum_{s_N} A_{s_1, s_2, \dots, s_N} |s_1\rangle \otimes |s_2\rangle \otimes \cdots \otimes |s_N\rangle$$

$$\approx \sum_{s_1} \sum_{s_2} \cdots \sum_{s_N} A_{s_1; \alpha_1}^1 A_{s_2; \alpha_1, \alpha_2}^2 \cdots A_{s_N; \alpha_{N-1}}^N |s_1\rangle \otimes |s_2\rangle \otimes \cdots \otimes |s_N\rangle$$



Truncate  $\alpha_i \leq D \forall i$

## Contractions

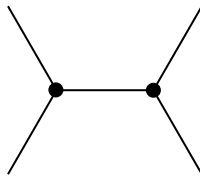
$$d = 1$$



=



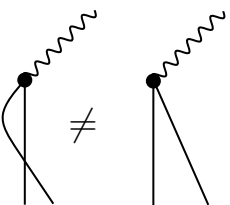
$$d > 1$$



=



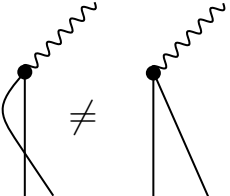
## Fermionic PEPS [Corboz et al. PRB 81 (2010)]

$$c_i c_k = -c_k c_i$$


A diagram illustrating the fermion commutation relation  $c_i c_k = -c_k c_i$ . It features two vertices connected by a horizontal wavy line. The left vertex has two lines entering from below and one line exiting to the right. The right vertex has one line entering from below and two lines exiting to the right. A diagonal line connects the top-left line of the left vertex to the bottom-right line of the right vertex. A horizontal line connects the bottom-left line of the left vertex to the top-right line of the right vertex. The two vertices are enclosed in a large oval.

$\neq$

## Fermionic PEPS [Corboz et al. PRB 81 (2010)]

$$c_i c_k = -c_k c_i$$
$$(c_i c_j) c_k = c_k (c_i c_j)$$


A diagram illustrating fermion commutation relations. It features two vertices connected by a horizontal line. The left vertex has two outgoing lines: one going up-right and another going down-left. The right vertex has two outgoing lines: one going up-left and another going down-right. A wavy line connects the two vertices. Below the diagram is a large inequality symbol ( $\neq$ ), indicating that the two configurations represent different states due to fermion statistics.

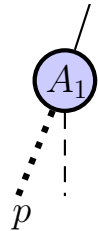
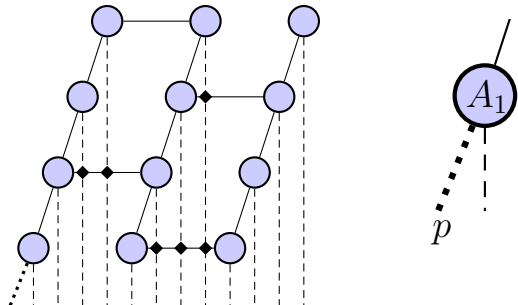
# Fermionic PEPS [Corboz et al. PRB 81 (2010)]

$$c_i c_k = -c_k c_i$$

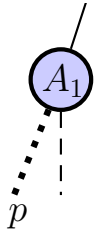
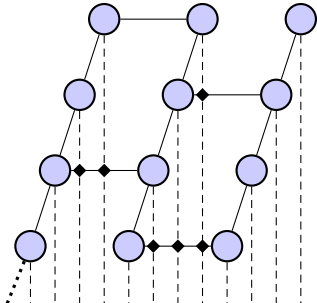
$$(c_i c_j) c_k = c_k (c_i c_j)$$

$$S = \left( \begin{array}{cccccc} 1 & \dots & 1 & 1 & \dots & 1 \\ \vdots & \ddots & \vdots & \vdots & \ddots & \vdots \\ 1 & \dots & 1 & 1 & \dots & 1 \\ 1 & \dots & 1 & -1 & \dots & -1 \\ \vdots & \ddots & \vdots & \vdots & \ddots & \vdots \\ 1 & \dots & 1 & -1 & \dots & -1 \end{array} \right) \left. \begin{array}{l} \text{even} \\ \text{odd} \end{array} \right\} \begin{array}{l} \text{even} \\ \text{odd} \end{array}$$

## Parity link



## Parity link



$p = \pm 1$   
⇒ even- and odd-parity  
subspaces are disjoint

## Ground state search

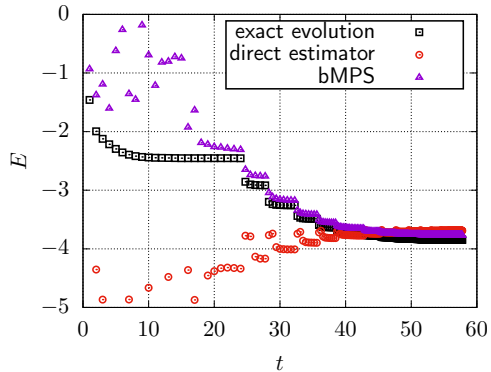
- ▶ Fix bond dimension  $D$

## Ground state search

- ▶ Fix bond dimension  $D$
- ▶ Initialise PEPS randomly

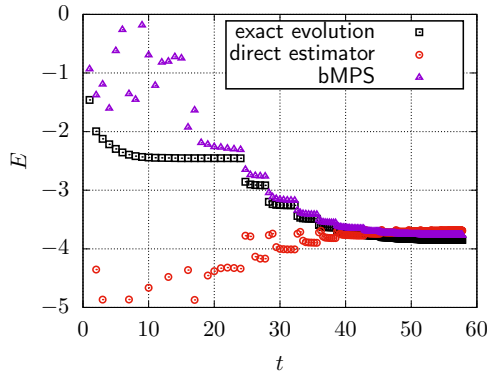
## Ground state search

- ▶ Fix bond dimension  $D$
- ▶ Initialise PEPS randomly
- ▶ Trotter-decomposed imaginary time evolution



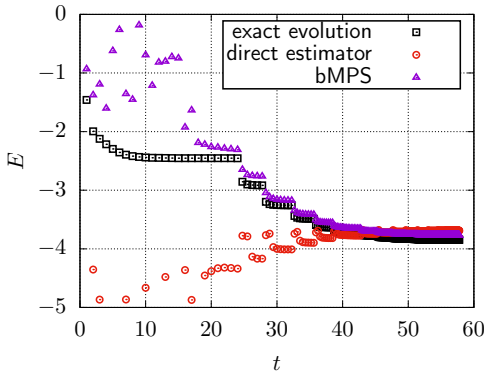
## Ground state search

- ▶ Fix bond dimension  $D$
- ▶ Initialise PEPS randomly
- ▶ Trotter-decomposed imaginary time evolution
- ▶ Local updates

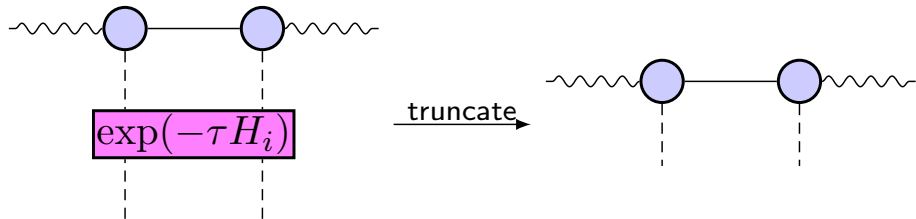


## Ground state search

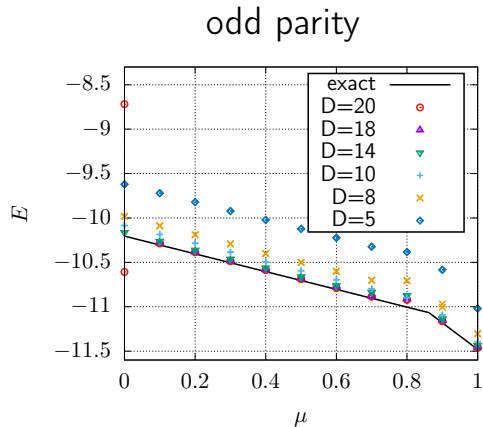
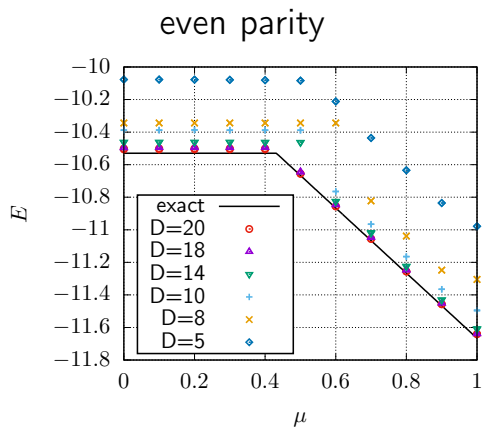
- ▶ Fix bond dimension  $D$
- ▶ Initialise PEPS randomly
- ▶ Trotter-decomposed imaginary time evolution
- ▶ Local updates
- ▶ Contract network to calculate expectation values



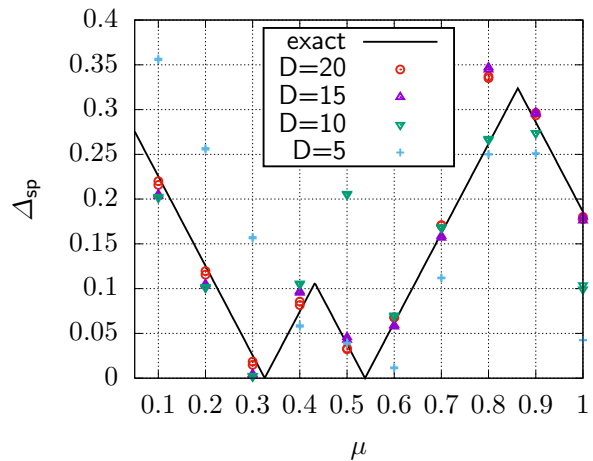
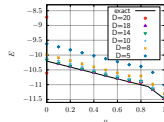
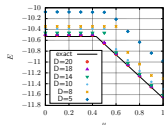
## Simple Update



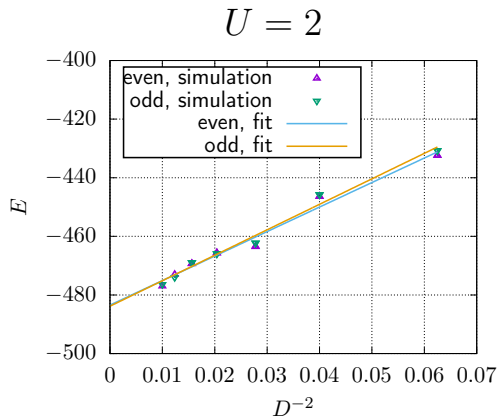
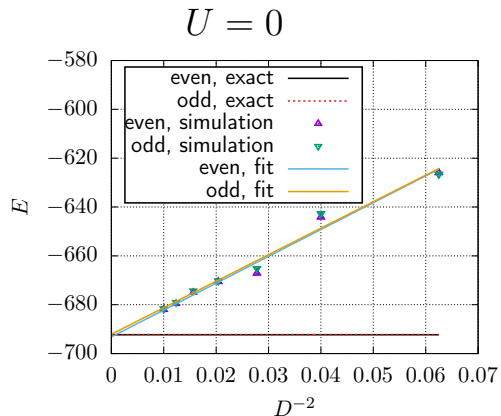
# Simulations with chemical potential ( $3 \times 4$ hex. lattice, $U = 2$ )



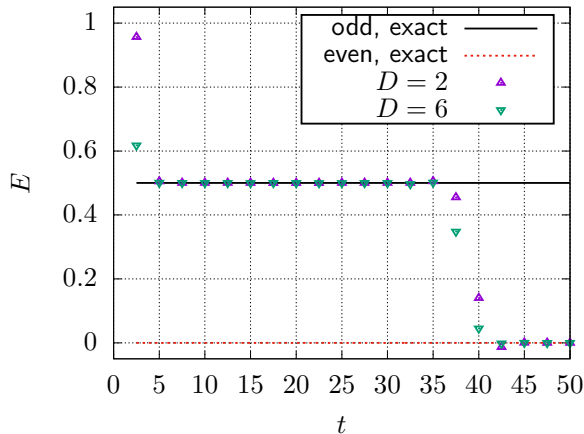
# Simulations with chemical potential ( $3 \times 4$ hex. lattice, $U = 2$ )



# Simulations with chemical potential ( $30 \times 15$ hex. lattice, $\mu = 0.5$ )

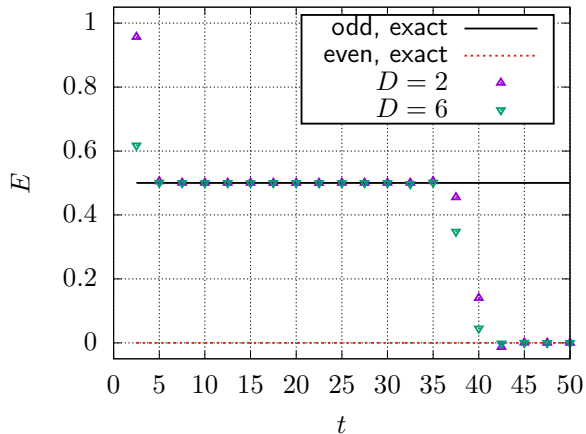


## Stability issues with odd parity



$3 \times 4$  hex. lattice,  $U = 1$ , no hopping

## Stability issues with odd parity



$3 \times 4$  hex. lattice,  $U = 1$ , no hopping

Large gap (strong coupling)  
⇒ jump to even parity  
ground state

## Overview

Hybrid Monte Carlo

Fermionic PEPS

## Overview

	Hybrid Monte Carlo	Fermionic PEPS
lattice size	$L \lesssim 100$	$L \lesssim 30$

## Overview

	Hybrid Monte Carlo	Fermionic PEPS
lattice size	$L \lesssim 100$	$L \lesssim 30$
boundary conditions	periodic	open

## Overview

	Hybrid Monte Carlo	Fermionic PEPS
lattice size	$L \lesssim 100$	$L \lesssim 30$
boundary conditions	periodic	open
thermodynamic limit	easy	hard

## Overview

	Hybrid Monte Carlo	Fermionic PEPS
lattice size	$L \lesssim 100$	$L \lesssim 30$
boundary conditions	periodic	open
thermodynamic limit	easy	hard
continuum limit	controlled, expensive	easy

## Overview

	Hybrid Monte Carlo	Fermionic PEPS
lattice size	$L \lesssim 100$	$L \lesssim 30$
boundary conditions	periodic	open
thermodynamic limit	easy	hard
continuum limit	controlled, expensive	easy
temperature	only finite	only zero

## Overview

	Hybrid Monte Carlo	Fermionic PEPS
lattice size	$L \lesssim 100$	$L \lesssim 30$
boundary conditions	periodic	open
thermodynamic limit	easy	hard
continuum limit	controlled, expensive	easy
temperature	only finite	only zero
other extrapolations	no	uncontrolled in $D$

## Overview

	Hybrid Monte Carlo	Fermionic PEPS
lattice size	$L \lesssim 100$	$L \lesssim 30$
boundary conditions	periodic	open
thermodynamic limit	easy	hard
continuum limit	controlled, expensive	easy
temperature	only finite	only zero
other extrapolations	no	uncontrolled in $D$
excited states	few lowest, expensive	some specific, instabilities

## Overview

	Hybrid Monte Carlo	Fermionic PEPS
lattice size	$L \lesssim 100$	$L \lesssim 30$
boundary conditions	periodic	open
thermodynamic limit	easy	hard
continuum limit	controlled, expensive	easy
temperature	only finite	only zero
other extrapolations	no	uncontrolled in $D$
excited states	few lowest, expensive	some specific, instabilities
sign problem	yes	no

## Overview

	Hybrid Monte Carlo	Fermionic PEPS
lattice size	$L \lesssim 100$	$L \lesssim 30$
boundary conditions	periodic	open
thermodynamic limit	easy	hard
continuum limit	controlled, expensive	easy
temperature	only finite	only zero
other extrapolations	no	uncontrolled in $D$
excited states	few lowest, expensive	some specific, instabilities
sign problem	yes	no
performance	CPU-intensive	RAM-intensive

## Full comparison of results

Method	$U_c/\kappa$	$\nu$	$\beta$
Grand canonical BRS HMC [JO, Berkowitz <i>et al.</i> <i>PRB</i> <b>104</b> (2021)]	3.834(14)	1.185(43)	1.095(37)
Grand canonical BSS HMC [Buividovich <i>et al.</i> 2018]	3.90(5)	1.162	1.08(2)
Grand canonical BSS QMC [Buividovich <i>et al.</i> 2019]	3.94	0.93	0.75
Projection BSS QMC [Otsuka <i>et al.</i> 2016]	3.85(2)	1.02(1)	0.76(2)
Projection BSS QMC [Otsuka <i>et al.</i> 2020]		1.05(5)	
Projection BSS QMC [Parisen Toldin <i>et al.</i> 2015]	3.80(1)	0.84(4)	0.71(8)
Projection BSS QMC [Liu <i>et al.</i> 2019]		0.88(7)	
Projection BSS QMC [Assaad & Herbut 2013]	3.78	0.882	0.794
GN $4 - \epsilon$ , 1st order [Herbut <i>et al.</i> 2009]		0.882	0.794
GN $4 - \epsilon$ , 1st order [Rosenstein <i>et al.</i> 1993]		0.851	0.824
GN $4 - \epsilon$ , 2nd order [Rosenstein <i>et al.</i> 1993]		1.01	0.995
GN $4 - \epsilon, \nu$ 2nd order [Rosenstein <i>et al.</i> 1993]		1.08	1.06
GN $4 - \epsilon, 1/\nu$ 2nd order [Rosenstein <i>et al.</i> 1993]		1.20	1.17
GN $4 - \epsilon, \nu$ 4th order [Zerf <i>et al.</i> 2017]		1.2352	
GN $4 - \epsilon, 1/\nu$ 4th order [Zerf <i>et al.</i> 2017]		1.5511	
GN FRG [Janssen & Herbut 2014]		1.31	1.32
GN FRG [Knorr 2018]		1.26	
GN Large $N$ [Gracey 2018]		1.1823	

## Bibliography I

-  Alexandru, A., Basar, G. & Bedaque, P. Monte Carlo algorithm for simulating fermions on Lefschetz thimbles. *Phys. Rev. D* **93**, 014504. arXiv: 1510.03258 [hep-lat] (*PRD* **93** (2016)).
-  Assaad, F. F. & Herbut, I. F. Pinning the order: the nature of quantum criticality in the Hubbard model on honeycomb lattice. *Phys. Rev. X* **3**, 031010.  
<https://link.aps.org/doi/10.1103/PhysRevX.3.031010> (2013).
-  Buividovich, P., Smith, D., Ulybyshev, M. & von Smekal, L. Hybrid Monte Carlo study of competing order in the extended fermionic Hubbard model on the hexagonal lattice. *Phys. Rev. B* **98**, 235129. <https://link.aps.org/doi/10.1103/PhysRevB.98.235129> (2018).
-  Buividovich, P., Smith, D., Ulybyshev, M. & von Smekal, L. Numerical evidence of conformal phase transition in graphene with long-range interactions. *Phys. Rev. B* **99**, 205434. arXiv: 1812.06435 [cond-mat.str-el] (2019).

## Bibliography II

-  Corboz, P. Improved energy extrapolation with infinite projected entangled-pair states applied to the two-dimensional Hubbard model. *Physical Review B* **93**. ISSN: 2469-9969 (*PRB* **93** (2016)).
-  Corboz, P., Orús, R., Bauer, B. & Vidal, G. Simulation of strongly correlated fermions in two spatial dimensions with fermionic projected entangled-pair states. *Phys. Rev. B* **81**, 165104 (16 *PRB* **81** (2010)).
-  Cristoforetti, M., Di Renzo, F., Mukherjee, A. & Scorzato, L. Monte Carlo simulations on the Lefschetz thimble: Taming the sign problem. *Phys. Rev. D* **88**, 051501. arXiv: 1303.7204 [hep-lat] (*PRD* **88** (2013)).
-  Fischer, JO, M., Kostrzewa, B., Otnad, K., Ueding, M. & Urbach, C. On the generalised eigenvalue method and its relation to Prony and generalised pencil of function methods. *Eur. Phys. J. A* **56**, 206 (*EPJ A* **56** (2020)).
-  Gracey, J. Large  $N$  critical exponents for the chiral Heisenberg Gross-Neveu universality class. *Phys. Rev. D* **97**, 105009. arXiv: 1801.01320 [hep-th] (2018).

## Bibliography III

-  Herbut, I. F., Juricic, V. & Roy, B. Theory of interacting electrons on the honeycomb lattice. *Phys. Rev. B* **79**, 085116. arXiv: 0811.0610 [cond-mat.str-el] (*PRB* **79** (2009)).
-  Herbut, I. F., Juricic, V. & Vafek, O. Relativistic Mott criticality in graphene. *Phys. Rev. B* **80**, 075432. arXiv: 0904.1019 [cond-mat.str-el] (2009).
-  Hills, G. et al. Modern microprocessor built from complementary carbon nanotube transistors. *Nature* **572**, 595–602 (*Nature* **572** (2019)).
-  Hubbard, J. Electron correlations in narrow energy bands. *Proceedings of the Royal Society of London A: Mathematical, Physical and Engineering Sciences* **276**, 238–257. ISSN: 0080-4630. eprint:  
<http://rspa.royalsocietypublishing.org/content/276/1365/238.full.pdf>.  
<http://rspa.royalsocietypublishing.org/content/276/1365/238> (*ProcRSoc* **276** (1963)).

## Bibliography IV

-  Janssen, L. & Herbut, I. F. Antiferromagnetic critical point on graphene's honeycomb lattice: A functional renormalization group approach. *Phys. Rev. B* **89**, 205403.  
<https://link.aps.org/doi/10.1103/PhysRevB.89.205403> (20 2014).
-  JO, Berkowitz, E., Krieg, S., Lähde, T. A., Luu, T. & Urbach, C. Semimetal–Mott insulator quantum phase transition of the Hubbard model on the honeycomb lattice. *Phys. Rev. B* **102**, 245105 (24 PRB **102** (2020)).
-  JO, Berkowitz, E., Krieg, S., Lähde, T. A., Luu, T. & Urbach, C. The Antiferromagnetic Character of the Quantum Phase Transition in the Hubbard Model on the Honeycomb Lattice. *Phys. Rev. B* **104**, 155142 (15 PRB **104** (2021)).
-  Knorr, B. Critical chiral Heisenberg model with the functional renormalization group. *Phys. Rev. B* **97**, 075129. arXiv: 1708.06200 [cond-mat.str-el] (2018).
-  Kostrzewa, JO, B., Ueding, M. & Urbach, C. *hadron: Analysis Framework for Monte Carlo Simulation Data in Physics*. R package version 3.1.0 (CRAN (2020)).  
<https://CRAN.R-project.org/package=hadron>.

## Bibliography V

-  Krieg, JO, S., Luu, T., Papaphilippou, P. & Urbach, C. Accelerating Hybrid Monte Carlo simulations of the Hubbard model on the hexagonal lattice. *Computer Physics Communications* **236**, 15 –25. ISSN: 0010-4655 (*CPC 236* (2019)).
-  Liu, Y. et al. Superconductivity from the Condensation of Topological Defects in a Quantum Spin-Hall Insulator. *Nature Commun.* **10**, 2658. arXiv: 1811.02583 [cond-mat.str-el] (2019).
-  Luu, T. & Lähde, T. A. Quantum Monte Carlo calculations for carbon nanotubes. *Phys. Rev. B* **93**, 155106. <https://link.aps.org/doi/10.1103/PhysRevB.93.155106> (15 PRB **93** (2016)).
-  Orús, R. A practical introduction to tensor networks: Matrix product states and projected entangled pair states. *Annals of Physics* **349**, 117–158. ISSN: 0003-4916 (*AnnPhys 349* (2014)).
-  Otsuka, Y., Seki, K., Sorella, S. & Yunoki, S. Dirac electrons in the square lattice Hubbard model with a  $d$ -wave pairing field: chiral Heisenberg universality class revisited. arXiv: 2009.04685 [cond-mat.str-el] (Sept. 2020).

## Bibliography VI

-  Otsuka, Y., Yunoki, S. & Sorella, S. Universal Quantum Criticality in the Metal-Insulator Transition of Two-Dimensional Interacting Dirac Electrons. *Phys. Rev. X* **6**, 011029 (2016).
-  Parisen Toldin, F., Hohenadler, M., Assaad, F. F. & Herbut, I. F. Fermionic quantum criticality in honeycomb and  $\pi$ -flux Hubbard models: Finite-size scaling of renormalization-group-invariant observables from quantum Monte Carlo. *Phys. Rev. B* **91**, 165108. arXiv: 1411.2502 [cond-mat.str-el] (2015).
-  Rodekamp, J.O., Berkowitz, E., G  ntgen, C., Krieg, S. & Luu, T. *Mitigating the Hubbard Sign Problem with Complex-Valued Neural Networks*. arXiv **2203** (2022). <https://arxiv.org/abs/2203.00390>.
-  Rosenstein, B., Yu, H.-L. & Kovner, A. Critical exponents of new universality classes. *Phys. Lett. B* **314**, 381–386 (1993).
-  Schneider, J.O., Jansen, K., Luu, T. & Urbach, C. Simulating both parity sectors of the Hubbard Model with Tensor Networks. *Phys. Rev. B* **104**, 155118 (15 PRB **104** (2021)).

## Bibliography VII

-  Ulybyshev, M., Winterowd, C. & Zafeiropoulos, S. Lefschetz thimbles decomposition for the Hubbard model on the hexagonal lattice. *Phys. Rev. D* **101**, 014508. arXiv: 1906.07678 [cond-mat.str-el] (*PRD* **101** (2020)).
-  Verstraete, F. & Cirac, J. I. Renormalization algorithms for Quantum-Many Body Systems in two and higher dimensions. *arXiv e-prints*, cond-mat/0407066. arXiv: cond-mat/0407066 [cond-mat.str-el] (July arXiv **0407066** (2004)).
-  Wallace, P. R. The Band Theory of Graphite. *Phys. Rev.* **71**, 622–634. <https://link.aps.org/doi/10.1103/PhysRev.71.622> (9 *PhysRev* **71** (1947)).
-  Wonen, J.-L., Berkowitz, E., Krieg, S. & Luu, T. Machine learning to alleviate Hubbard-model sign problems. *Phys. Rev. B* **103**, 125153 (12 *PRB* **103** (2021)).
-  Zerf, N., Mihaila, L. N., Marquard, P., Herbut, I. F. & Scherer, M. M. Four-loop critical exponents for the Gross-Neveu-Yukawa models. *Phys. Rev. D* **96**, 096010. arXiv: 1709.05057 [hep-th] (2017).